

Cationic Polymerization of *p*-Methoxystyrene in Miniemulsion

S  verine Cauvin, Amel Sadoun, Rosalina Dos Santos, Jo  l Belleney, Fran  ois Ganachaud,* and Patrick Hemery

Laboratoire de Chimie des Polym  res, UMR 7610 CNRS/Universit   Pierre et Marie Curie, T44 E1, 4 Place Jussieu, 75252 Paris Cedex, France

Received February 21, 2002; Revised Manuscript Received July 10, 2002

ABSTRACT: The cationic polymerization of *p*-methoxystyrene (pMOS) in miniemulsion in the presence of dodecylbenzenesulfonic acid (DBSA) was studied. DBSA acts as both protonic initiator and surfactant (INISURF). The recipe was first optimized to generate stable latexes from a miniemulsion, i.e., droplets/particles of constant size throughout the polymerization. The miniemulsion polymerization process was highly reproducible, quite fast at high temperatures (100% conversion in 8 h at 60   C) and applicable even at high monomer content (typically 40 wt %). Poly(pMOS) of small average molar masses (≈ 1000 g mol⁻¹) and controlled functionality were synthesized. The sharp increase in molar masses at low conversion was indebted to a decrease of water content at the interface through a cosurfactant effect. Above 20% conversion, the chain length limitation, also observed in previous ionic polymerizations in emulsion studies and referred to as critical DP, was confirmed by modeling simple kinetics. At final conversion, polymer degradation occurred as revealed by SEC, MALDI-TOF, and ¹H NMR. The particles quickly coalesced in the absence of a cosurfactant.

Introduction

Ionic polymerization in emulsion (IPE) is an original process to generate nanoparticles from heterocyclic^{1–7} and vinyl monomers.^{8–10} Preparation of poly(dimethylsiloxane) latexes by cationic and anionic polymerizations of cyclosiloxane in *emulsion* have been known for 40 years in industry,^{1,2} whereas polymerizations of *mini-emulsion* were primarily academic studies.^{3–6} Indeed, the formation of “ready-to-go” droplets facilitated mechanistic studies by avoiding the complex particle nucleation step. Kinetic studies showed that the chain propagation at the interface occurred principally at low conversion.⁶ Termination by water¹¹ was also substantial, but this reaction is reversible, thus allowing chains to grow. Condensation and redistribution reactions were retarded but still occurred at high conversion. A far less reactive heterocyclic monomer, phenyl glycidyl ether (PGE), has also been polymerized anionically in mini-emulsion.⁷ IPE likely applies to alkyl cyanoacrylates that react spontaneously in water to generate nanoparticles.^{8,9} Excess acid (pH 2–3) improved the control of cyanoacrylate polymerization in the emulsion by inducing fast but reversible termination; i.e., most of the chains were dormant.⁹ Both systems obey a simple kinetic scheme; i.e., initiation, propagation, and termination reactions take place at the interface.

A recent study reported the controlled polymerization of *p*-methoxystyrene (pMOS) in a suspension using sulfonic acids as initiators and a rare earth salt (ytterbium triflate) as a catalyst.¹⁰ The authors proposed that dormant sulfonyl-terminated chains were activated by the few ytterbium triflate molecules penetrating the monomer droplets to generate long-lived polymer chains (see Scheme 1 in ref 10). Controlled polymerization could be achieved up to 25% conversion, after which a pseudo-plateau in molar mass variations with conversion was reached. This loss of control presumably arose from transfer reactions with water.¹¹

These results prompted us to use such rare-earth catalyst in a miniemulsion process. We chose a sulfonic acid surfactant i.e., dodecylbenzenesulfonic acid (DBSA), in place of previous sulfonic acids to stabilize the particles and to favor inner or interfacial initiation reactions. Preliminary blank experiments showed that the polymerization took place *in the absence of ytterbium triflate*. The present study deals with physicochemical and kinetic aspects of pMOS cationic polymerization in miniemulsion using DBSA as an INISURF (initiator/surfactant).

Experimental Part

Materials. Unless otherwise stated, all reagents were purchased from Acros. *p*-Methoxystyrene (pMOS, 99%) was used as supplied. The purity of dodecylbenzenesulfonic acid (DBSA, Janssen Chimica, 98%) was confirmed by ¹H and ¹³C NMR before use. Pentanol, 3-ethyl-3-pentanol, and 1-methoxy-naphthalene (all 98% purity) were used as received. Solvents for analyses, i.e., CDCl₃ (Euriso Top), THF (Prolabo), as well as CH₂Cl₂ (Carlo-Erba), used for polymer extraction, were of analytical grade (purity above 99.5%). 2,5-Dihydroxybenzoic acid (DHB, Aldrich, 98%) was used as a matrix for MALDI-TOF analyses.

Methods. ¹H NMR measurements were carried out on a Br  ker AC 200 spectrometer in CDCl₃ at room temperature, using the following conditions: spectral width 30 ppm with 16K data points, flip angle of 15  , relaxation delay of 1.4 s, digital resolution of 0.36 Hz/pt. The chemical shift scale was calibrated relative of the solvent peak (7.24 ppm).

Particle size measurements were performed on a Zetasizer 4 from Malvern Instruments. Samples were diluted in a solution of DBSA (4.4×10^{-4} mol L⁻¹) below its critical micellar concentration ($\text{cmc} = 1.2 \times 10^{-3}$ mol L⁻¹ from ref 12) prior analysis. Particle sizes are expressed as *z*-average diameters.

Size exclusion chromatography (SEC) measurements were carried out on a device composed of a 515 HPLC pump (Waters), an autosampler S5200 (Viscotek), and a differential refractometer S200 (Viscotek). Three columns (one column with 10^{2.5}    pore size, two mixed-bed columns of average pore sizes 10⁴ and 10⁵   , all from Shodex) thermostated at 30   C were eluted with THF at a flow rate of 1 mL min⁻¹. The calibration curve was made from polystyrene standards (between 264 and 67 500 g mol⁻¹, from Viscotek).

* To whom correspondence should be addressed: Tel 33 1 44 27 55 01; Fax 33 1 44 27 70 89; e-mail ganachau@ccr.jussieu.fr.

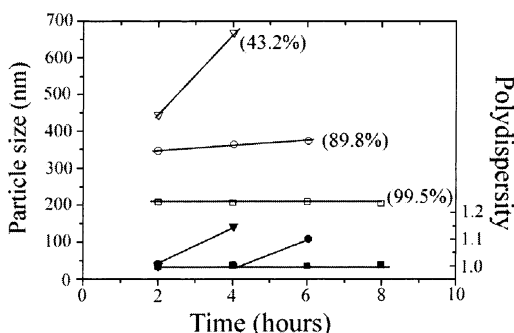


Figure 1. Influence of the INISURF amount on miniemulsion stability vs time (open symbol, hydrodynamic particle diameter; close symbol, size distribution polydispersity index). Surfactant content (wt % compared to monomer): (∇) 2, (\circ) 5, (\square) 10 (Table 1, runs 1, 2, and 3, respectively). Values in parentheses indicate at which conversion the emulsion starts to visually destabilize. Lines are only guides for the eyes.

MALDI-TOF mass spectrometry analyses were performed on a PerSeptive Biosystems Voyager Elite (Framingham, MA) time-of-flight mass spectrometer, equipped with a nitrogen laser (337 nm–3 ns pulse), a delayed extraction, and a reflector. It was operated at an accelerating potential of 20 kV in reflected mode. The polymer solution (10 μ L of 1 g L⁻¹ in THF) was mixed with 20 μ L of the matrix solution (DHB, 20 g L⁻¹ in THF) and 10 μ L of a sodium iodide solution (20 g L⁻¹ in THF), which favors ionization by cation attachment. The final solution (1 μ L) was deposited onto the sample target and dried in air at room temperature before irradiation. The MALDI mass spectra represent averages over 256 consecutive laser shots (3 Hz repetition rate). Polystyrene standards were used to calibrate the mass scale using the two-point calibration software from PerSeptive Biosystems.

Polymerization in Miniemulsion. Miniemulsions were prepared by ultrasound sonication using a 450 Branson Ultrasonics Corp. sonifier at power 7 (25 W). Typically, 3.2 g of pMOS (2.4 mmol) was added to the surfactant solution (0.32 g of DBSA, 1 mmol, in 8 g water, 0.4 mol) maintained at a temperature of 25 °C using an ice bath during sonication (1 min 30 s). The emulsion was then transferred into the reactor, where polymerization proceeded under thermal regulation (40 °C) and mechanical stirring (350 rpm). Polymerization was completed after 2 days.

At regular time intervals, 2 mL aliquots were withdrawn and neutralized with a stoichiometric amount of 0.1 N NaOH solution to stop the polymerization. A few drops of the emulsion were used to measure the particle diameter. A spatula of aluminum salt (AlK₂S₂O₈·12H₂O, Acros Organics, 99.5%) and 1 mL of CH₂Cl₂ were then added to the remaining sample to achieve easy phase separation by centrifugation and to ensure that no organic products remained in water.

The monomer conversion was determined by ¹H NMR and SEC analyses (see Figure 2a). ¹H NMR showed the decrease of the vinyl peaks at 5.64 and 5.72 ppm compared to the aromatic broad peak around 7 ppm. For SEC measurements, monomer conversion was calculated from monomer and polymer peak integration, taking into account their respective refractive indexes (1.562 and 1.570). SEC traces and average molar mass variations are given in Figures 3 and 2b, respectively.

Results

All surfactant concentrations are expressed in weight percent compared to monomer throughout the paper.

Stability Criteria for Polymerizing pMOS Miniemulsions. It was shown previously that cyclosiloxane miniemulsions were easily prepared due to the high hydrophobicity of these monomers (on the order of 10⁻⁷ mol L⁻¹),¹³ whereas those containing more polar mono-

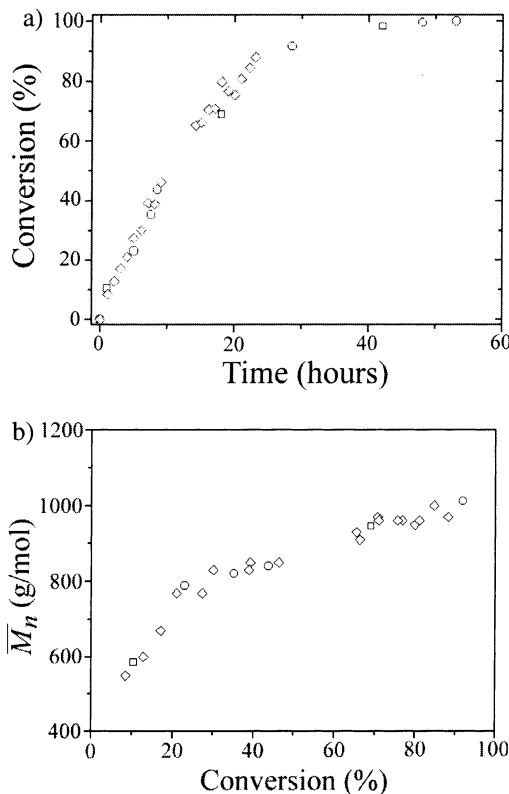


Figure 2. Cationic polymerization of pMOS in miniemulsion for a model system (40 °C, 28 wt % monomer) for three different runs (see Table 1, runs 4 (\square), 5 (\circ), and 6 (\diamond)): (a) conversion–time curve; (b) average molar mass variation with conversion.

mers such as PGE were difficult to stabilize prior and during polymerization.⁷

Figure 1 reports the evolution of hydrodynamic particle size and size distribution polydispersity index (PDI) for experiments prepared with various amounts of DBSA (Table 1, runs 1–3). The miniemulsion prepared with 2 wt % surfactant (Table 1, run 1) exhibits large particle size from the beginning and quickly coalesces (a latex can be considered broad for PDI above 1.10; see Figure 1). Besides, 10 wt % surfactant (Table 1, run 3) conducts to stable particles of usual size for miniemulsions prepared by ultrasonication (typically 200 nm).

The two major processes of destabilization of emulsions are coalescence and Ostwald ripening.¹⁴ The former generally occurs at low surfactant concentration; 10 wt % of DBSA is thus necessary to sustain the latex stability. The second process involves monomer diffusion from the small particles to the larger ones due to their different osmotic pressures. The addition of a hydrophobic molecule¹⁵ cancels particle ripening by virtually increasing the inner-particle osmotic pressure of small droplets. Such a destabilization process does not seem to take place here as the particle size remains constant throughout the polymerization (Figure 1). Furthermore, addition of 1-methoxynaphthalene (hydrophobe strongly compatible with pMOS) affects neither the particle size nor the polymerization rate (Table 1, run 12; compare to run 3). The fact that miniemulsions does not require the addition of a hydrophobe while performing IPE is understood from the polymerization mechanism. Droplet nucleation through interfacial initiation starts as soon as the system is sonified. The few polymer chains

Table 1. Recipes and Main Results for All Experiments Reported in This Paper^a

run	w_{pMOS}^b (g)	w_{DBSA}^b (g)	$w_{\text{H}_2\text{O}}^b$ (g)	temp (°C)	monomer content (%)	particle size ^d (nm)	PDI ^d	polymerization rate ^e (wt %/h)	final \overline{M}_n (g mol ⁻¹)
1	3	0.06	5	60	35	<i>e</i>	<i>e</i>	10.6	<i>e</i>
2	3	0.15	5	60	37	350	1.004	16.9	1050
3	2.4	0.24	4	60	36	208	1.003	25.8	1060
4	3.2	0.32	8	40	28	<i>f</i>	<i>f</i>	4.5	1000
5	2.4	0.24	6	40	28	<i>f</i>	<i>f</i>	4.5	1000
6	5.6	0.56	14	40	28	240	1.006	4.5	1000
7	3	0.3	15	25	16	<i>f</i>	<i>f</i>	2.2	1055
8	4	0.4	10	25	28	215	1.005	2.2	1100
9	3.6	0.36	6	25	36	200	1.020	2.2	1230
10	3	0.3	5	40	37	<i>f</i>	<i>f</i>	4.7	1150
11	4	0.4	10	60	28	<i>f</i>	<i>f</i>	22.5	985
12 ^c	2.4	0.24	4	60	28	195	1.009	28.0	905
13 ^c	2.4	0.24	4	60	28	270	1.003	13.6	670
14 ^c	2.4	0.24	4	60	28	250	1.004	21.9	900

^a All ingredients were mixed at 25 °C, ultrasonified, and poured in a reactor before setting the temperature (variable) and agitation (350 rpm). ^b w = weight content. pMOS = *p*-methoxystyrene; DBSA = dodecylbenzenesulfonic acid. ^c Runs carried out in the presence of an additive (10 wt % compared to monomer): methoxynaphthalene (run 12), pentanol (run 13), 3-ethyl-3-pentanol (run 14). ^d Measured by QELS. ^e From the slope at the origin on the conversion/time curve. ^f Instable particles (see Figure 1). ^g Not determined.

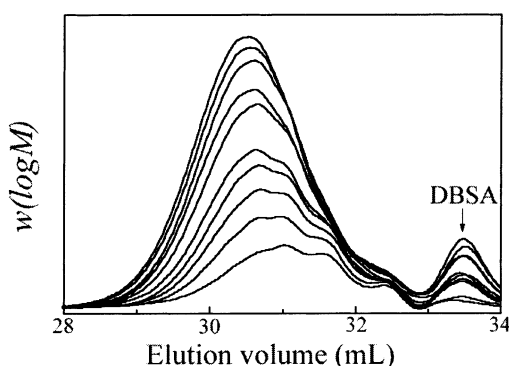


Figure 3. SEC traces of pMOS polymerization for increasing conversion (Table 1, run 6). From bottom to top (% conversion): 21.0, 30.1, 38.9, 46.2, 51.7, 66.3, 70.7, 79.9, 84.7, and 88.1.

generated at the beginning of the polymerization act as hydrophobes and thus suppress Ostwald ripening.

The knowledge of particle size and particle size evolution is primordial in IPE. Indeed, initiation reaction takes place at the interface, and the polymerization rate is thus directly related to the specific surface displayed by the latex. In most conditions, the particle size does not vary with conversion, albeit above 20% conversion; when available, some average particle sizes are reported in Table 1.

Main Features of pMOS Miniemulsion. *Model Polymerization.* Figure 2a shows the kinetic curves from three different experiments for a typical miniemulsion (40 °C, 28 wt % monomer content; see Table 1, runs 4–6). A very good reproducibility is observed between each experiments. The final conversion reaches 100%, but the reaction is quite slow (about 2 days to reach final completion at 40 °C).

Figure 2b plots the average molar mass \overline{M}_n as a function of conversion obtained from the SEC distributions and using a polystyrene calibration curve. The average molar mass rises quickly up to 800 g mol⁻¹ (20% conversion) and then gradually up to about 1000 g mol⁻¹ (eight monomer units).

SEC traces of various samples normalized by their conversion are shown in Figure 3 (Table 1, run 6). The bumps in the SEC distribution correspond to isolated oligomers of at least three units (compare with DBSA peak in Figure 3). The peak maximum shifts with conversion, though distributions still overlap in the low

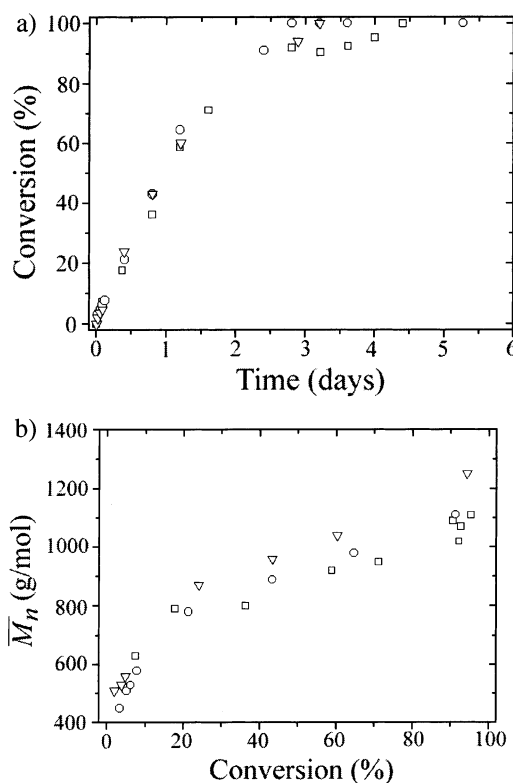


Figure 4. Influence of monomer content on (a) conversion vs time plot and (b) average molar masses vs conversion plot. $T = 25$ °C. Monomer content (wt %): (□) 16, (○) 28, and (▽) 36 (Table 1, runs 7, 8, and 9, respectively).

molar mass range. The content of DBSA extracted from the CH_2Cl_2 /aluminum salt procedure (see Experimental Part) also increases with conversion.

Weight Content. Figure 4a reports conversion–time curves at various monomer contents and constant monomer/surfactant ratio at 25 °C (Table 1, runs 7–9). A SEC peak due to CH_2Cl_2 used during the polymer extraction overlaps with that of monomer. At low monomer content and high conversion, SEC conversion measurements are thus prone to uncertainties (see Figure 4a). There are no striking variations in polymerization rate between these experiments. The evolution of average molar mass with conversion is reported Figure 4b. The final molar masses are slightly larger at high monomer content, as already observed (however

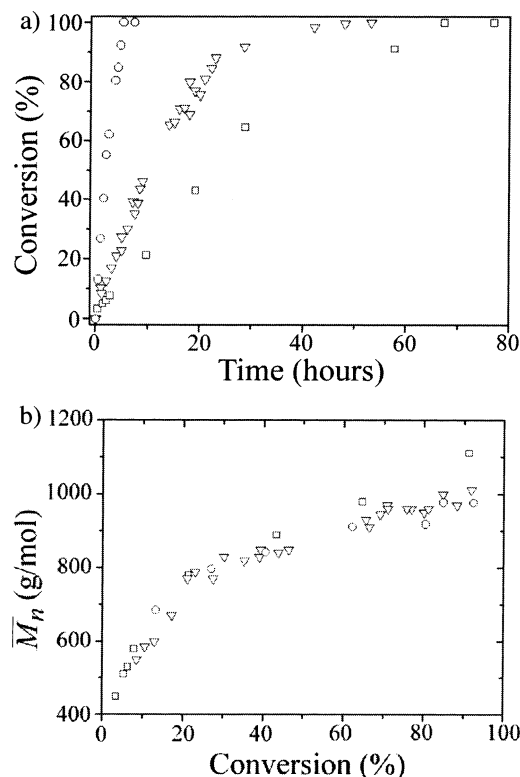


Figure 5. Influence of temperature on (a) conversion vs time plot and (b) average molar masses vs conversion plot. Monomer content 27 wt %. Temperature (°C): (□) 25, (▽) 40, and (○) 60 (Table 1, runs 8, 6, and 11, respectively).

to a greater extent) in the cationic polymerization in miniemulsion of 1,3,5,7-tetramethylcyclotetrasiloxane (D_4H).⁵

Temperature Effect. Parts a and b of Figure 5 report the effect of temperatures (25, 40, and 60 °C) on polymerization rate and molar mass variations, respectively, using 27 wt % monomer (Table 1, runs 6, 8, and 11). Increasing temperature significantly enhances the polymerization rate: complete polymerization of pMOS is achieved in 8 h at 60 °C (run 11), whereas about 1 and 3 days are necessary at 40 (run 6) and 25 °C (run 8), respectively. Because particle sizes are close (Table 1), the variation in specific surface is not the main reason for polymerization rate enhancement with temperature. Most certainly, propagation rate increases with temperature as observed in PGE polymerization.⁷ The molar mass evolutions with conversion are however similar.

Surfactant Content. Increasing the surfactant concentration decreases the average particle size of the miniemulsion (Figure 1). The conversion–time curve and average molar masses are presented in parts a and b of Figure 6, respectively, for two surfactant concentrations (Table 1, runs 3 and 2, 10 and 5 wt % surfactant, respectively). Polymerization is slower at the lowest acid content as expected from the larger particle size and lower initiator amount. pH measurements were also carried out to estimate the degree of INISURF coverage at the interface. Figure 7 shows an example for 10 wt % DBSA (Table 1, run 3). The pH decreases with conversion to reach a plateau at 20–30% conversion, after which very few protons are available at the interface for initiating the polymerization.

Cosurfactant Effect. Table 1 shows the average particle size and polydispersity of the particles, the polymerization rate, and final average molar masses in the

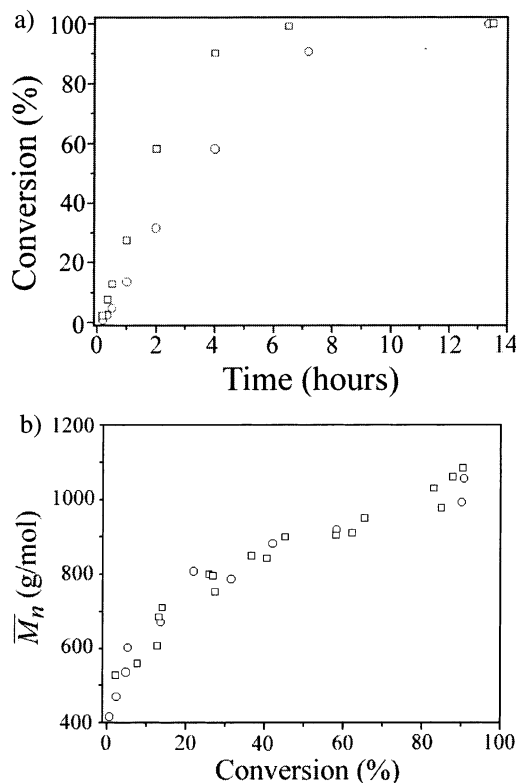


Figure 6. Influence of surfactant concentration on (a) conversion vs time plot and (b) average molar masses vs conversion plot. Surfactant concentrations (wt % compared to monomer): (○) 5 and (□) 10 (Table 1, runs 2 and 3, respectively).

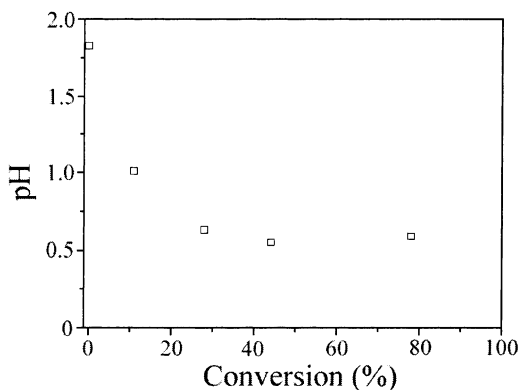


Figure 7. pH variation as a function of conversion at 60 °C and 37 wt % monomer content (Table 1, run 3).

presence of small alcohol cosurfactants, pentanol or 3-ethyl-3-pentanol (runs 13 and 14, respectively). Particle sizes with both additives were slightly larger than for the original latex (Table 1, run 3). The molar mass evolution with conversion is reported in Figure 8. Pentanol reacts with active species to give pentoxy-functionalized oligomers of very low molar masses (DP 3 or 4). Once it is consumed, longer chains are generated (above 60% conversion, Figure 8). Consequently, the polymerization rate halved compared to the original miniemulsion polymerization (termination rather than transfer reaction occurs; see ref 11). A tertiary alcohol, e.g., 3-ethyl-3-pentanol, avoids chain stopping: the polymerization rate is similar to original emulsion, and molar masses vary with conversion (Figure 8). The chains reached however a plateau at lower average molar masses (about 860 g mol⁻¹) than without additive because of different interface polarities (see Discussion).

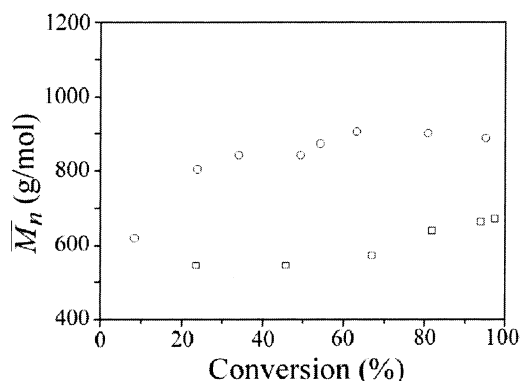


Figure 8. Influence of cosurfactant addition on the average molar masses vs conversion plot. $T^{\circ} = 60^{\circ}\text{C}$, monomer content = 37 wt %. Additives (10 wt % compared to monomer): (\square) pentanol and (Δ) 3-ethyl-3-pentanol (Table 1, runs 13 and 14, respectively).

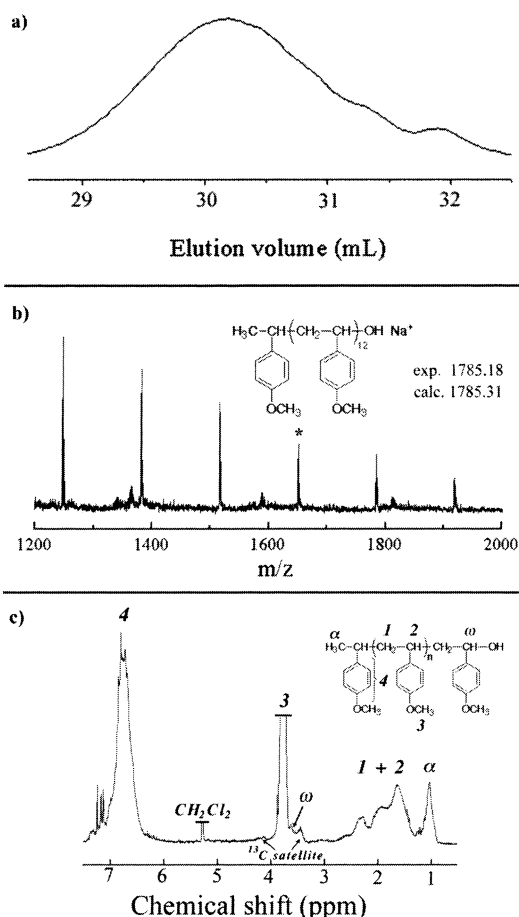


Figure 9. Polymer chain characterization of a sample withdrawn at almost 100% conversion for polymerization set at 60°C and 28 wt % monomer content (Table 1, run 11): (a) SEC trace; (b) MALDI-TOF spectrum. The calculated and theoretical molar masses are also reported in the graph. (c) ^1H NMR spectrum and assignments for the main chain groups and extremities. The broad polymer methoxy peak was truncated so that to see end-group peaks.

Polymer Characterization. Chain-End Analyses. Figure 9 shows the SEC, MALDI-TOF, and ^1H NMR spectra of a polymer withdrawn at almost 100 wt % conversion (Table 1, run 11). MALDI-TOF analysis shows that all chains bear one methyl and one hydroxyl chain end provided by proton initiation and water termination, respectively. Side reactions such as transfer to monomer, which would have generated ethylenic

or indanyl terminations, are clearly absent during the polymerization of PMOS in the emulsion process. The IPE peculiarity of generating fully functionalized chains was already addressed in previous PGE⁷ or cyclosiloxane⁶ studies.

The ^1H NMR spectrum of the same sample is reported in Figure 9. Apart from the main polymer peaks assigned in the figure, the methyl moiety shows up at 1 ppm, and the CH near the OH ω -extremity is located below the large methoxy peak at approximately 3.7 ppm. Note that the peak at 4.14 ppm was misleadingly assigned to the CH moiety in Sawamoto's study,¹⁰ which in turn explains their discrepancies in integration of both extremity peaks. This peak, with its counter pendant at 3.44 ppm, actually corresponds to the ^{13}C satellites of the polymer methoxy group.¹⁶ Finally, some small resolved peaks around the aromatic peak indicate that some degradation reactions start to occur when the polymerization is finished (see below).

Molar Masses Using Various Techniques. The average molar masses can be calculated independently from ^1H NMR, SEC, and MALDI-TOF, with the latter providing absolute values. For the sample characterized above (Figure 9), \overline{M}_n of 750, 960, and 1160 g mol^{-1} were respectively found. The ^1H NMR value is calculated from integrating the well-resolved α , rather than ω , end peak against the aromatic multiplet. Small amounts of DBSA extracted with the polymer (see Figure 3) and showing up below the CH_3 peak definitely account for the underestimated molar mass using NMR. The SEC method also systematically led to smaller molar masses than using MALDI-TOF. Quantitative SEC analyses of oligomers prepared by IPE are difficult to perform because their hydroxyl end groups affect both the $d n/dc$ and their elution response.¹⁷ Higher elution volume for small oligomers bearing OH extremities, prone to interact with the columns, were recently observed for silanol compared to trimethyl-terminated PDMS standards.⁶ Since the difference between MALDI and SEC was less than 20%, no correction was made in this paper.

Chain Degradation after Polymerization. Once the monomer is totally consumed, the excess acid present in the dispersion ($\text{pH} = 0.6$) regenerates carbocations that participate to degradation reactions.

SEC, MALDI-TOF, and ^1H NMR spectra for the same experiments as before, but on a sample withdrawn 3 days after polymerization ceased, are plotted in Figure 10 (Table 1, run 11).

The SEC trace clearly shifted toward higher elution volume, i.e., lower molar masses. MALDI-TOF revealed at first sight a dehydration of the chains, which cannot be indebted to the technique as shown from the nondegraded polymer spectrum (Figure 9). A closer look on spectrogram further shows that the distribution of degraded polymer is also shifted toward smaller molar masses (see the envelopes between nondegraded and degraded chains, Figure 10). The ^1H NMR spectrum after degradation revealed the generation of numerous resolved peaks in the 6 and 7.5 ppm regions, confirming the conversion of chain ends into ethylenic and indanyl moieties (see assignments, Figure 10).

To summarize, chain-end dehydration, as well as chain scission, is responsible for the generation of short chains during the acid-catalyzed degradation reactions of poly(PMOS). More thorough investigations are clearly out of the scope of this study; for further details,

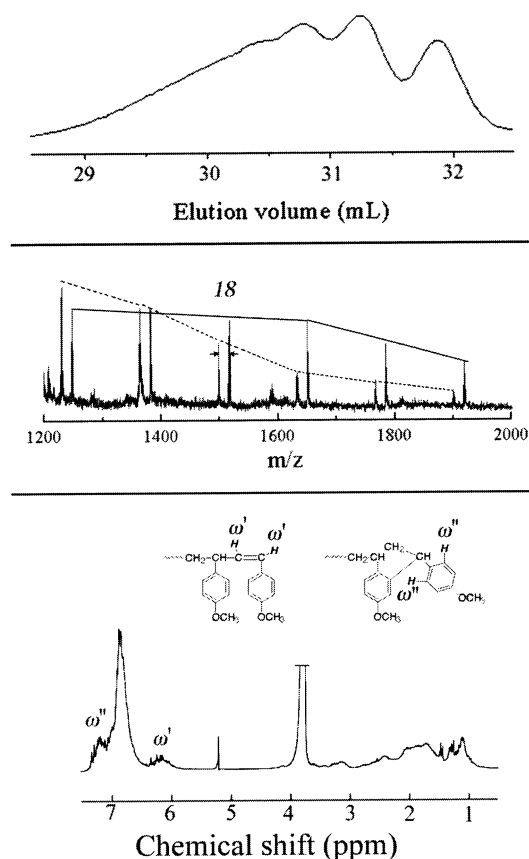


Figure 10. Same analyses than in Figure 9, but for a sample maintained 3 days at 60 °C after polymerization ceased: (a) SEC trace; (b) MALDI-TOF spectrum. Also reported in the graph are the envelopes of nondegraded (solid line) and degraded (dashed line) chains. (c) ¹H NMR spectrum and assignments of peaks typical of degraded extremities.

however, the reader is directed to the extensive work of Moreau on the subject.¹⁸

A direct consequence of polymer degradation is a fast coagulation of the emulsion. Similar poor stability was observed in the PGE polymerization in miniemulsion that contained mainly short surface-active oligomers.⁷ The addition of the alcohol cosurfactant allows for better stability of the emulsion, though not precluding final chain degradation. The fact that the acid does not degrade this tertiary alcohol may explain the increased

emulsion stability. Another way to keep the particles stable consists of preventing polymer degradation by neutralizing the emulsion typically at 95% conversion.

Discussion¹⁹

Ionic polymerization in miniemulsion proceeds at the particle interface.⁷ Polymerization is initiated by a proton, and the resultant active center associates with the pendant sulfonate moiety. The protected ion pair propagates further until water terminates growth and regenerates the proton (Scheme 1).

This basic scheme cannot explain the increase in molar masses with conversion. Either *reversible* termination or *decreasing* termination may rationalize such a trend. The former implicates that controlled polymerization occurs, whereas the latter recalls an interface modification.

Termination Reaction. Controlled Termination. Reversible termination was asserted in the study on pMOS polymerization in suspension in the presence of ytterbium triflate.¹⁰ The deviation from the theoretical curve for molar mass variations was attributed to both slow initiation rate and chain transfer reactions.²⁰ Similar behavior in the present system would indicate that sulfonic acid is strong enough to reactivate the chains during the polymerization. This result is consistent with the reformation of carbocation, which is responsible for polymer degradation, once the polymerization ceases.

The initiation reaction is related to the formation of the chains N as a function of time t :

$$R_i = dN/dt = k_i[H^+][M] \quad (1)$$

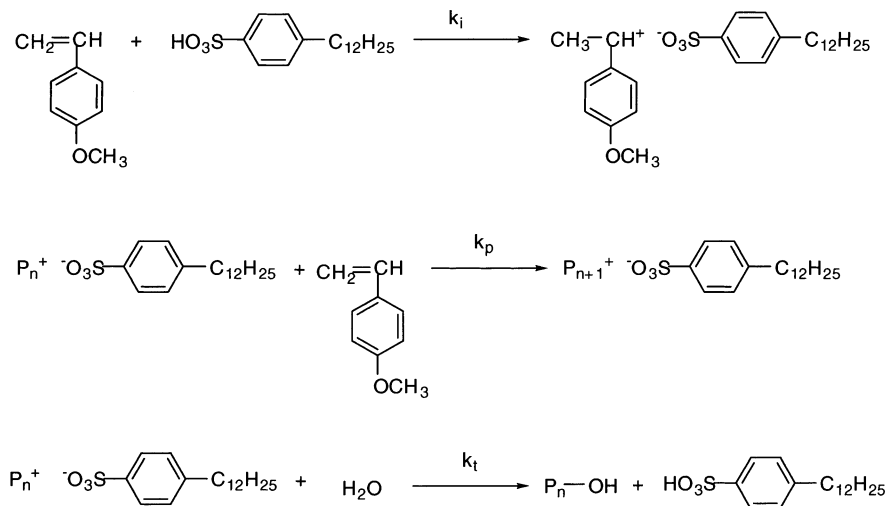
where $[H^+]$ and $[M]$ stand for protons and monomer concentrations at time t , respectively. N (in mol L⁻¹) is deduced from SEC measurements by

$$N = ([M]_0 - [M]) / \overline{DP}_n \quad (2)$$

where $[M]_0$ is the initial monomer concentration and \overline{DP}_n the average degree of polymerization at time t .

N as a function of time plot is reported in Figure 11 (Table 1, run 6). The initiation rate is low and decreases with conversion. The chains could be reactivated, the consequence of which would be a complete shift of the

Scheme 1



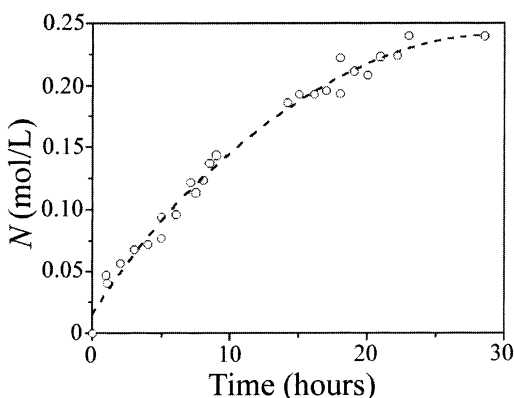


Figure 11. Molar concentration of chains N vs time for model experiment, i.e., 40 °C, 28 wt % monomer (Table 1, run 6). The line is only guide for the eyes.

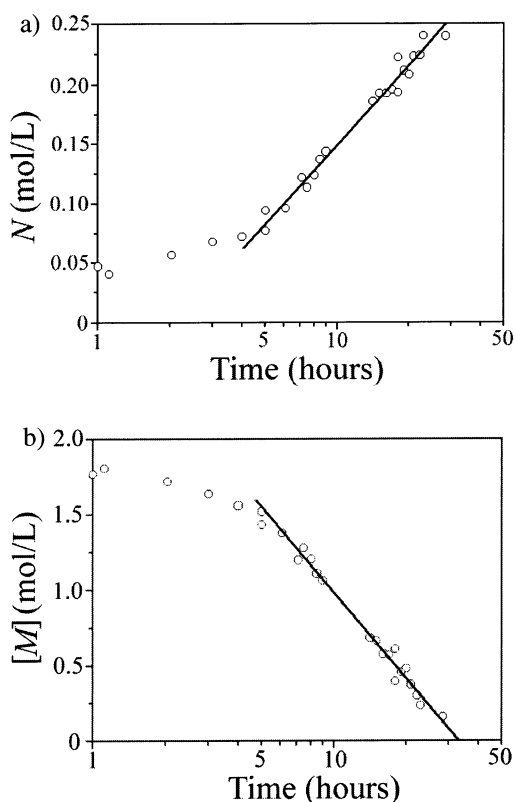


Figure 12. Semilog plot of (a) N vs time (reprocessed from Figure 11); (b) $[M]$ vs time (reprocessed from Figure 2a) for model experiment (40 °C, 28 wt % monomer, Table 1, run 6). Best linear fits are also reproduced in the plots.

polymer distribution toward high molar masses at increasing conversion. Such a trend is clearly not seen in the SEC traces, which have a low molar mass tail (Figure 3).

Another argument against reversible termination is given in Figure 6b, where the average molar mass as a function of conversion is plotted for two different INISURF concentrations. Longer chains should be generated at smaller acid amount, which is clearly not observed from these experimental data.

Cosurfactant Effect. The main reason for molar mass increase with conversion is thus indebted to a decrease of termination reaction. In our previous publication on PGE anionic polymerization in miniemulsion,⁷ polyPGE oligomers were shown to protrude at the interface by their carbinol functionality. Water content at the inter-

face decreased, and hence longer chains were synthesized at increasing conversion. A similar cosurfactant effect is proposed here for the pMOS system. Small oligomers generated at the beginning of the polymerization are not reactivated, which is revealed by the overlap in SEC traces (Figure 3). Intrusion of hydroxylated poly(pMOS) at the interface provokes a release of DBSA in the water phase and a decrease of the pH (Figure 7). It also partly expels water from the interface, which allows longer chains to be generated. Such a cosurfactant effect however ends at about 20% conversion, at which the new initiated chains rapidly reach the critical DP and enter the particle (Figure 2b).

Critical DP. *Experimental Fact.* A striking feature in ionic polymerization in emulsion processes is the systematic limitation of the molar masses. This so-called "critical DP" effect was related to the entry in the particles of chains with low surface tensions.⁶ Once buried, they stop propagating. The anionic polymerization in emulsion of octamethylcyclotetrasiloxane (D_4) produced chains of typically 2500 g mol^{-1} ,^{3,6} regardless of the temperature or monomer and surfactant contents. Similar features applied to other cyclosiloxanes (e.g., F_3^6). For cyanoacrylate^{8,9} or PGE,⁷ the critical DP was found to be twice smaller than for cyclosiloxanes. This is presumably due to the difference in surface tensions of silanol and carbinol. The cyanoacrylate system clearly outlines the unique feature of IPE process, where chains of typically 1200 g mol^{-1} ^{8,9} should be compared to those of a few million g mol^{-1} produced in bulk or solution polymerization!²¹ Analogously, the poly(pMOS) chains do not stay at the interface for molar masses above 800 g mol^{-1} . This behavior is illustrated by the significant break observed in the molar mass variation at 20% conversion.

\overline{M}_n still slowly increases above 20% conversion because the small chains generated at the beginning of the polymerization weigh on the overall distribution.²² Similar to cyclosiloxanes, the critical DP is not affected by the temperature because it is independent of rate constants. Increasing the monomer content decreases the interfacial water content (Figure 4b) and generates slightly longer chains.

Kinetics Modeling. The modeling is carried out for data at conversions greater than 20%, at which the emulsion features are unchanged. The average DP is calculated from the kinetical chain length expression:

$$\overline{DP}_{\text{kin}} = R_p/R_t \quad (3)$$

where R_p and R_t are the propagation and termination rates, respectively.

Slow initiation and rapid irreversible termination allow to apply the steady-state approximation, i.e.

$$d[P^+]/dt = R_i - R_t \approx 0 \quad (4)$$

with $[P^+]$ the concentration of active chains. Equation 3 becomes

$$\overline{DP}_{\text{kin}} = R_p/R_i \quad (5)$$

where

$$R_p = k_p[P^+][M] \quad (6)$$

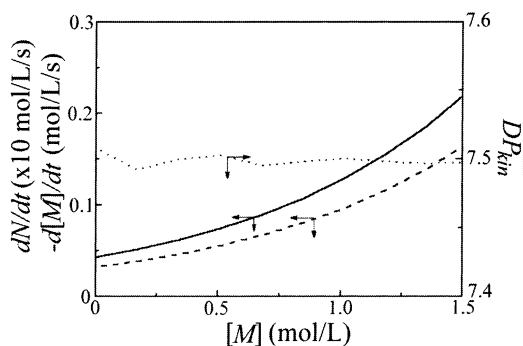


Figure 13. Best-fitted dN/dt (solid line) and $-d[M]/dt$ (dashed line) as well as \overline{DP}_{kin} (dotted line) as a function of monomer concentration $[M]$ reprocessed from Figure 13 (see text for details).

and R_t as given in eq 1. \overline{DP}_{kin} simplifies to

$$\overline{DP}_{kin} = k_p[P^+]/k_t[H^+] \quad (7)$$

The method followed to extract \overline{DP}_{kin} at different conversions is given in the Appendix. Though both $k_p[P^+]$ and $k_t[H^+]$ decrease with monomer consumption, their ratio remains constant with time (see Figure 13). The theoretical molar mass of 1030 g mol^{-1} is very close to what was experimentally observed here (Figure 2b).

Complementary Issues. To summarize, the IPE process permits to synthesize oligomers whose molar masses are controlled by the interfacial polarity. For reversible termination, all chains rapidly grow to the critical DP prior to entering the particles; if termination is nonreversible, small oligomers accumulate at the interface before the new chains reach the critical DP.

The generation of long chains in IPE should be feasible for emulsion with exceptionally low surface polarity. The addition of short alcohol produced smaller chains than in the original miniemulsion (Figure 8b, to be compared to Figure 2b), contrary to what was observed in PGE polymerization.⁷ The obtained molar masses depend in fact on the polarity of the short alcohols compared to the cosurfactant oligomers (mono- and dihydroxylated for pMOS and PGE, respectively), i.e., of the water content at the interface. Increasing the hydrophobicity of the surfactant and/or cosurfactant is thus a key parameter for increasing the molar masses in IPE.

Finally, for systems exhibiting nonreversible termination, such as pMOS or PGE,⁷ it is necessary to ensure rapid propagation before chain stopping. "Slow" monomers could a priori polymerize in dispersed media using efficient and water-tolerant catalysts, such as zinc or cadmium salts for episulfide anionic polymerization²³ or ytterbium triflate in cationic polymerization.¹⁰

Conclusion

pMOS was polymerized in the presence of a sulfonic acid surfactant and without ytterbium triflate catalyst. Polymerization takes place at the interface, similar to the IPE systems published previously. Although poly-(pMOS) average molar mass increases with conversion, this cannot be due to "controlled" active center generation. Besides, the early oligomer chains act as cosurfactants and decrease termination by expelling water from the interface. The occurrence of a critical DP, as

observed in previous systems, was confirmed by simple kinetic modeling.

Compared to the present study, suspension pMOS polymerization in the presence of ytterbium triflate had similar conversion and molar mass evolutions with time.¹⁰ Longer chains ($\approx 4 \times 10^3 \text{ g mol}^{-1}$) were however generated. The interfacial process proposed here may account for these results, rather than a controlled polymerization. Ytterbium triflate favors quick propagation by stretching the sulfonate/carbocation ion pair. In addition, the presence of a high load of ytterbium salt is likely to decrease the water content at the interface, thus increasing the critical DP. We are currently seeking conditions for polymerizing pMOS in the presence of ytterbium triflate and in *miniemulsion* and further checking on these issues.²⁴

Acknowledgment. This work was supported by a grant from ADEME and Rhodia Recherches. F.G. greatly acknowledges B. Charleux, M. Moreau, M. Barrère, and A. Elaissari for helpful comments on the manuscript.

Appendix¹⁹

According to eq 7, \overline{DP}_{kin} can be calculated from $k_t[H^+]$ and $k_p[P^+]$ variations. The former is obtained from the dN/dt vs $[M]$ curve (see eq 1). The N vs t curve plotted in Figure 11, though comprising many data, generated scattered curve while performing direct derivation. The N vs t plot was then fitted with an exponential curve, which has no physical meaning but is easy to derive (Figure 12a). The derivative of this fitted curve is plotted as a function of monomer concentration (Figure 13, solid line).

The second term is inferred from the monomer consumption with time given by

$$-d[M]/dt = R_i + R_p = (k_p[P^+] + k_t[H^+])[M] \quad (8)$$

Again, the $[M]$ against t plot (from Figure 2a) is best fitted with an exponential curve (Figure 12b) whose derivative is plotted as a function of $[M]$ (Figure 13, dashed line). The resulting \overline{DP}_{kin} vs $[M]$ curve is also given in Figure 13 (dotted line).

Note that both exponential curves fit the data for polymerization time above 5 h, e.g., conversion above 20%, as proposed in the Discussion.

References and Notes

- Hyde, J. F.; Wehrly, J. R. Dow Corning Corporation, U.S. Patent 2891920, 1959.
- Gee, R. P. Dow Corning Corporation, European Patent 0459500, 1991.
- De Gunzburg, A.; Favier, J.-C.; Hémerly, P. *Polym. Int.* **1994**, *35*, 179.
- De Gunzburg, A.; Maisonnier, S.; Favier, J.-C.; Maitre, C.; Masure, M.; Hémerly, P. *Macromol. Symp.* **1998**, *132*, 359.
- Maisonnier, S.; Favier, J.-C.; Masure, M.; Hémerly, P. *Polym. Int.* **1999**, *48*, 159.
- Barrère, M.; Ganachaud, F.; Bendejacq, D.; Dourges, M.-A.; Maitre, C.; Hémerly, P. *Polymer* **2001**, *42*, 7239.
- Maitre, C.; Ganachaud, F.; Ferreira, O.; Lutz, J.-F.; Paintoux, Y.; Hémerly, P. *Macromolecules* **2000**, *33*, 7730.
- Behan, N.; Birkinshaw, C. *Macromol. Rapid Commun.* **2000**, *21*, 884.
- Behan, N.; Birkinshaw, C.; Clarke, N. *Biomaterials* **2001**, *22*, 1335.
- Satoh, K.; Kamigaito, M.; Sawamoto, M. *J. Polym. Sci., Part A* **2000**, *38*, 2728.
- Strictly speaking, water attack on the siloxide should be considered a transfer reaction, as the regenerated hydroxyl anion can initiate a new chain. However, because of the low

- efficiency of this initiator and the high water content at the interface, the term termination is more appropriate to describe the water behavior (see: Matyjaszewski, K.; Pugh, C. In *Cationic Polymerizations: Mechanisms, Synthesis, and Applications*; Matyjaszewski, K., Ed.; Marcel Dekker: New York, 1996; p 250).
- (12) Zweltloot, L. J. *Colloid Interface Sci.* **1995**, *175*, 1.
 - (13) Lee Smith, A.; Parker, R. D. In *Trace Analysis Involving Silicones*; Lee Smith, A., Ed.; John Wiley & Sons: New York, 1991; p 83.
 - (14) Sudol, E. D. E.; El-Aasser, M. S. In *Miniemulsion Polymerization*; Lovell, P. A., El-Aasser, M. S., Eds.; John Wiley & Sons: New York, 1997; p 699.
 - (15) Landfester, K. *Macromol. Rapid Commun.* **2001**, *22*, 896.
 - (16) 0.35 ppm separates the main methoxy peak from both satellite, which corresponds to a coupling constant of 140 Hz at 200 MHz, very close to the theoretical value (150 Hz). In addition, the relative abundance of ^{13}C against ^1H could not be better estimated than less than 1% for each, to be compared to the theoretical 0.55%.
 - (17) For more information on SEC oligomer analyses, see the following references: (a) Cook, S. D.; Sible, V. S. *Eur. Polym. J.* **1997**, *33*, 163. (b) Harrisson, C. A.; Mourey, T. H. *J. Appl. Polym. Sci.* **1995**, *56*, 211. (c) Gridnev, A. A.; Cottés, P. M.; Roe, C.; Barth, H. *J. Polym. Sci., Polym. Chem.* **2001**, *39*, 1099.
 - (18) Moreau, M. Ph.D. Thesis, Université Pierre et Marie Curie, 1988.
 - (19) This part relies on data from the most complete experiments, i.e., at 40 °C with 27 wt % monomer content (Table 1, run 6). As stated before, the system is a true miniemulsion; i.e., particle size does not vary with conversion (see Figure 1). Concentrations are thus expressed as bulk ones.
 - (20) For a recent and concise review, see: Qiu, J.; Charleux, B.; Matyjaszewski, K. *Polimery* **2001**, *7/8*, 453 and references therein.
 - (21) Ryan, B.; McCann, G. *Macromol. Rapid Commun.* **1996**, *17*, 217.
 - (22) One referee suggested that we worked out the variation of the polydispersity indexes, which low values would confirm the sharp cutoff in molar masses at the critical DP. Dead chains however accumulate right from the beginning and broaden the distribution. One would need to extract the "instantaneous" molar mass distributions, by normalizing and subtracting two SEC traces set at close conversion. This manipulation resulted in very noisy distributions that could not be exploited. Note however that, in the siloxane IPE process where termination is reversible, all chains reached the critical DP and the polydispersity indexes remained low at low conversion, i.e., before polycondensation reactions broaden the distribution. Extrapolation at zero conversion even gave a polydispersity of 1.01 (see ref 6).
 - (23) (a) Dunlop: British Patent 1,117,307, 1964. (b) Dunlop: British Patent, 1,123,801, 1965.
 - (24) The preliminary experiments tried out in our laboratory were not conclusive. Basically, ytterbium triflate greatly dissociated in water (70 wt % in a large concentration range) and implemented such a high ionic strength that the emulsion instantaneously broke, even at low catalyst content.

MA0202890